




A specialised SKI complex assists the cytoplasmic RNA exosome in the absence of direct association with ribosomes

Elodie Zhang^{1,2,†}, Varun Khanna^{1,3,†}, Estelle Dacheux¹, Abdelkader Namane¹ , Antonia Doyen¹, Maité Gomard¹, Bernard Turcotte⁴, Alain Jacquier^{1,*}  & Micheline Fromont-Racine^{1,**} 

Abstract

The Ski2-Ski3-Ski8 (SKI) complex assists the RNA exosome during the 3' to 5' degradation of cytoplasmic transcripts. Previous reports showed that the SKI complex is involved in the 3' to 5' degradation of mRNAs, including 3' untranslated regions (UTRs) and devoid of ribosomes. Paradoxically, we recently showed that the SKI complex directly interacts with ribosomes during the co-translational mRNA decay and that this interaction is necessary for its RNA degradation promoting activity. Here, we characterised a new SKI-associated factor, Ska1, that associates with a subpopulation of the SKI complex. We showed that Ska1 is specifically involved in the degradation of long 3'UTR-containing mRNAs, poorly translated mRNAs as well as other RNA regions not associated with ribosomes, such as cytoplasmic lncRNAs. We further show that the overexpression of SKA1 antagonises the SKI-ribosome association. We propose that the Ska1-SKI complex assists the cytoplasmic exosome in the absence of direct association of the SKI complex with ribosomes.

Keywords exosome; mRNA decay pathway; ribosome; *Saccharomyces cerevisiae*; SKI complex

Subject Categories RNA Biology

DOI 10.15252/embj.2018100640 | Received 4 September 2018 | Revised 25 April 2019 | Accepted 13 May 2019 | Published online 7 June 2019

The EMBO Journal (2019) 38: e100640

Introduction

RNA degradation is a key component of RNA homeostasis and quality control. During normal mRNA turnover, controlled deadenylation is followed by 5'-3' mRNA degradation by the cytoplasmic exonuclease Xrn1 as well as 3' to 5' degradation involving the cytoplasmic exosome (for reviews, see Fromont-Racine & Saveanu,

2014; Parker, 2012). In the major 5'-3' mRNA degradation pathway, mRNA deadenylation is followed by decapping by Dcp1/Dcp2 with the help of several enhancers of decapping such as Edc1, Edc2, Edc3, Dhh1, Pat1, Scd6 and the Lsm complex. This is followed by mRNA degradation *via* Xrn1, a co-translational process (Hu *et al*, 2009; Pelechano *et al*, 2015). The 3' to 5' mRNA degradation pathway involves the cytoplasmic exosome composed of 10 main factors, including the catalytically active subunit Dis3 (Allmang *et al*, 1999). Depending on its localisation, the exosome is assisted by different co-factors. The nuclear exosome associates with the distributive exoribonuclease Rrp6 as well as Mpp6, Lrp1/Rrp47 and the RNA helicase Mtr4, which is found within the TRAMP complex (Trf4/5, Air1/2, Mtr4; de la Cruz *et al*, 1998; Mitchell *et al*, 2003; Milligan *et al*, 2008). In the cytoplasm, the exosome is targeted to substrates by the SKI complex, composed of Ski2, Ski3 and Ski8 (SKIV2L, TTC37 and WDR61, respectively, in human).

The SKI genes were identified 40 years ago by performing a genetic screen with a yeast strain containing linear double-stranded RNAs encapsulated into virus-like particles secreting toxic proteins. Mutants having a deleterious phenotype were isolated and called SKI for super killer (Toh-E *et al*, 1978). Therefore, the first function reported for the SKI genes was in antiviral defence through viral RNA degradation (Widner & Wickner, 1993). Twenty years later, these genes were shown to be required for 3' to 5' mRNA degradation (Anderson & Parker, 1998) and to form a complex *in vivo* (Brown *et al*, 2000). Native mass spectrometry analyses revealed that the yeast SKI complex is a heterotetramer formed of one copy of Ski2 and Ski3 and two copies of Ski8 (Synowsky & Heck, 2008). Ski2 is an RNA helicase with a structure similar to the nuclear Mtr4 helicase. Ski8 contains WD40 repeats, while Ski3 is a tetratricopeptide repeat (TPR)-containing protein, which forms the scaffold of the SKI complex (Halbach *et al*, 2013). Ski2 is thought to be required to unwind RNA and to remove proteins bound to mRNAs. Ski3 and Ski8 contribute to the structure and activity of the SKI complex (Halbach *et al*, 2013). Although Ski7 is not part of the SKI

1 Génétique des Interactions Macromoléculaires, Institut Pasteur, UMR3525 CNRS, Paris, France

2 Sorbonne Université, Collège Doctoral, Paris, France

3 Hub Bioinformatique et Biostatistique, Institut Pasteur - C3BI, USR 3756 IP CNRS, Paris, France

4 Department of Medicine, McGill University Health Centre, Montréal, QC, Canada

*Corresponding author. Tel: +33 140 613 205; E-mail: jacquier@pasteur.fr

**Corresponding author. Tel: +33 140 613 432; E-mail: mfromont@pasteur.fr

†These authors contributed equally to this work

complex, it is also involved in mRNA 3' to 5' degradation (van Hoof *et al*, 2000) through bridging the SKI complex and the exosome (Araki *et al*, 2001). Interestingly, Ski7 interacts with the same exosome region as the nuclear factor Rrp6 (Kowalinski *et al*, 2016). Recently, structural data showed that the SKI complex forms a path for the RNA through a central channel of its helicase, Ski2. RNase protection assays performed with a mixture of the exosome and the SKI complex revealed protected fragments with a length compatible with a continuous channel formed by the SKI and the exosome complexes. It was proposed that the SKI complex directly delivers single-stranded RNA into the exosome (Halbach *et al*, 2013). Altogether, these results led to a model in which the cytoplasmic exosome and the SKI complex could be structurally organised to degrade RNA molecules, in a fashion similar to the proteasome involved in protein degradation (Halbach *et al*, 2013).

In addition to its role in the general mRNA degradation pathway, the SKI complex is also required for cytoplasmic mRNA surveillance pathways that are found in species ranging from yeast to human. These pathways are involved in the degradation of abnormal RNAs. These RNAs (i) may lack a Stop codon (Non-Stop mRNA decay, NSD), (ii) contain a premature Stop codon (Non-sense-mediated mRNA decay, NMD), and (iii) be bound by stalling ribosomes (No-Go mRNA decay, NGD; Frischmeyer, 2002; van Hoof *et al*, 2002; Mitchell & Tollervey, 2003; Doma & Parker, 2006). Recent *in vivo* and *in vitro* experiments have shown that the 3' to 5' mRNA degradation by the SKI-exosome complex is a co-translational event (Schmidt *et al*, 2016), in analogy to the Xrn1-dependent 5'-3' mRNA degradation pathway (Pelechano *et al*, 2015). This conclusion is supported by a series of observations: (i) affinity purification of a nascent peptide captured on ribosomes stalled at the end of a Non-Stop mRNA co-purifies ribosome associated with the SKI complex; (ii) a Ski3 affinity purification enriches ribosomes along with the SKI complex; (iii) these SKI-ribosome complexes are found associated with most open reading frames, as determined by footprinting experiments; (iv) the cryo-electron microscopy structure of the SKI-ribosome complex shows that the SKI complex interacts intimately with the small subunit of the ribosome. Notably, this interaction appears to be important to activate the Ski2 helicase by changing the conformation of two elements that autoinhibit the ATPase activity of the SKI complex. The arch domain of Ski2 moves away from the RNA helicase channel, and the N-terminal arm of Ski3 adopts a more open conformation (Schmidt *et al*, 2016). However, these observations are at odds with previous reports which showed that the SKI complex is required for the efficient degradation of 3'UTRs by the exosome (Anderson & Parker, 1998). Since 3'UTRs are essentially devoid of ribosomes, this implies that the SKI complex can act as an exosome co-factor without requiring an association with ribosomes. In an attempt to solve this paradox, we investigated the mechanism of action of the SKI complex on ribosome-free RNA regions.

Here, we have identified a new component of the yeast SKI complex that we called Ska1 for SKI-associated component 1. This protein is encoded by *YKLO23W*, a gene of unknown function. We demonstrated that this factor is not involved in the translation-dependent NSD pathway but rather in the general RNA degradation pathway, specifically in the degradation of RNA regions devoid of ribosomes. The SKI-Ska1 subcomplex is required for the 3' to 5' degradation of mRNA 3'UTR regions of poorly translated mRNAs

and long non-coding cytoplasmic RNAs (lncRNAs). Interestingly, Ska1 is not involved in the efficient degradation of coding mRNA regions or for the elimination of aberrant transcripts such as Non-Stop mRNAs. Overexpression of *SKA1* antagonises the association of the SKI complex with ribosomes, precluding its activity in degrading ribosome-associated RNA regions such as NSD substrates. These results suggest that, depending on the translation status of the RNA region being targeted, the SKI complex interacts either with the ribosome or Ska1. We thus propose that Ska1 allows the SKI complex to assist the cytoplasmic exosome in the absence of a direct association of the SKI complex with ribosomes.

Results

Ska1 is a novel factor associated with a subpopulation of the SKI complex

To investigate the mechanism of action of the SKI complex, we performed an affinity purification using Ski3-TAP as a bait. The proteins associated with Ski3-TAP were separated on a polyacrylamide gel (Fig 1A) and identified by mass spectrometry (LC-MS/MS). Analysis of the label-free quantitative MS data, represented by a volcano plot, showed the enrichment for three groups of proteins associated with Ski3 (Fig 1B). As expected, the most enriched proteins relative to the untagged strain control were the bait Ski3-TAP and the two other subunits of the SKI complex, Ski2 and Ski8. A second group was composed of the six RNasePH domain proteins of the exosome (Rrp41, Rrp42, Rrp43, Rrp45, Rrp46 and Mtr3), the catalytic subunit Dis3 and its three RNA-binding subunits (Rrp4, Rrp40 and Csl4). These factors form the 10-subunit cytoplasmic exosome (Fig 1B, in yellow; Liu *et al*, 2006). Ski7 and a novel factor of unknown function, Ykl023w, were also enriched at a similar level than the exosome subunits. We named the uncharacterised Ykl023w protein Ska1 for SKI-associated component 1 (Fig 1B). The third group of proteins was mainly related to the ribosome.

To confirm the physical interaction between Ska1 and the SKI complex, we performed affinity purification using a Ska1-TAP strain under the same conditions of purification used for Ski3-TAP (Fig 1C). We tested the functionality of the TAP fusions combining Ski3-TAP or Ska1-TAP with a *dcp2* degron fusion mutant (*dcp2d*) whose expression is negatively controlled by auxin (IAA; see below). We observed that Ski3-TAP, but not Ska1-TAP, was fully functional in this assay (Fig EV1). Indeed, in the presence of auxin, *dcp2d Ska1-TAP* cells grew faster than *dcp2d ska1Δ* cells but clearly slower than *dcp2d* single mutant cells (Fig EV1). Nevertheless, the analysis of label-free quantitative MS data revealed that the complex associated with Ska1 was highly similar to the SKI complex purification. We again observed an enrichment for three groups of proteins. The most enriched proteins were Ski2, Ski3 and Ski8, which were found at levels comparable to the Ska1-TAP bait. As observed with Ski3-TAP, the second group of proteins associated with Ska1-TAP was mainly related to the exosome and Ski7. The enrichment for the third group of proteins related to the ribosome was less important than the one observed with the Ski3-TAP purification.

To better evaluate the relative distribution of Ska1 and SKI components in the complexes, we looked at the relative protein

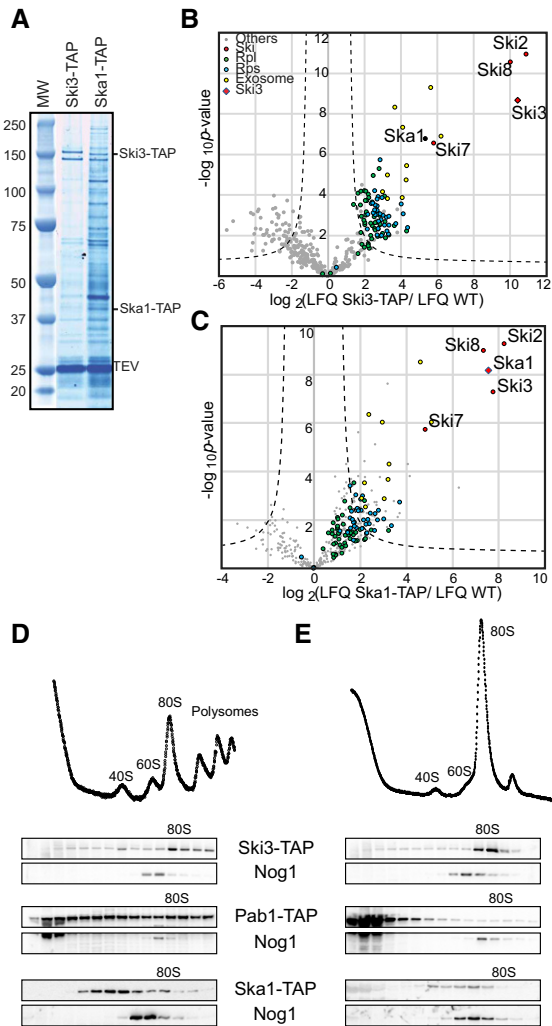


Figure 1. Ska1 is associated with the SKI complex.

- A Affinity purifications using Ska1-TAP and Ski3-TAP. The components of the TEV eluates were separated on a polyacrylamide NuPAGE Novex 4–12% Bis-Tris gel (Life Technologies) and visualised with Coomassie blue staining. MW, Molecular weight marker.
- B Statistical analysis of the fold enrichment of protein after one-step affinity purification using the Ski3-TAP as a bait (six replicates) followed by mass spectrometry analysis (LC-MS/MS). The enrichment was calculated relative to a control purification using the untagged reference strain BY4741 and represented, on the x-axis, as $\log_2(\text{LFQ Ski3-TAP/LFQ WT})$ where LFQ stands for label-free quantification (LFQ). The y-axis represents the *P*-value distribution ($-\log_{10} P\text{-value}$) calculated using the Student's *t*-test for all identified proteins represented by a circle. Red; the SKI complex; yellow, the exosome; blue, the small subunit ribosomal proteins—RPSs; green, the large subunit ribosomal proteins—RPLs. The red diamond indicates the protein used as a bait for the affinity purification. Proteins above the curved lines show a statistically significant enrichment according to the *t*-test value (see Dataset EV1).
- C Same as in (B) but for the Ska1-TAP purification (six replicates).
- D Total cellular extracts from cells expressing either Ski3-TAP or Ska1-TAP or Pab1-TAP were separated on a sucrose gradient (10–50%) by ultracentrifugation. Proteins of each fraction were analysed by Western blot using a PAP antibody for the detection of the TAP fusion protein and anti-Nog1 antibody to mark the 60S fraction.
- E Total cellular extracts were treated with RNase before loading on the sucrose gradient and analysed as in (D).

Source data are available online for this figure.

abundance in a wild-type yeast strain (Nagaraj *et al*, 2012). The analysis of 4,077 proteins revealed that Ska1 and components of the SKI complex were expressed at low levels. In addition, Ska1 was expressed to a level lower than the components of the SKI and exosome complexes (Fig EV2, upper panel). However, despite its lower abundance, Ska1 was enriched to a level comparable to the exosome components after purification of the complex associated with Ski3 (Fig EV2 middle panel). In addition, the Ski proteins were more enriched in the Ska1-TAP than the exosome (Fig EV2 lower panel). These results suggest that most of the Ska1 molecules are associated with the SKI complex. In contrast, only a fraction of the SKI complex is associated with Ska1.

Affinity purification showed that Ska1 was also associated with the ribosome, yet to a lesser extent compared to Ski3 (Fig 1B and C). To verify this association, we fractionated cellular extracts from a Ska1-TAP strain on a sucrose gradient. The analysis of the fractions by Western blot revealed that Ska1-TAP co-sediments with the 80S peak, the light polysomal fractions and lighter fractions in a region of the gradient where the 40S and 60S subunits sediment (Fig 1D). For comparison, a similar experiment performed with the Ski3-TAP strain showed a greater enrichment of Ski3 in the 80S peak, as previously described (Fig 1D; Schmidt *et al*, 2016). These observations are in agreement with the results of affinity purification showing a stronger association of Ski3-TAP than Ska1-TAP with the ribosome. To determine whether the weak association of Ska1 with the 80S ribosome and polysomes was direct or mRNA-mediated, we performed a RNase treatment of Ska1-TAP, Ski3-TAP cellular extracts before their fractionation on a sucrose gradient (Fig 1E). We used Pab1-TAP as a mRNA-binding protein control. As expected, RNase treatment resulted in the disappearance of the polysomes and the accumulation of 80S monosomes. After RNase treatment, Ski3-TAP still co-sedimented with the 80S ribosome, as previously shown (Schmidt *et al*, 2016), whereas Pab1-TAP, which was distributed all along the sucrose gradient in the absence of RNase, sedimented in the light fractions as a free protein, confirming the efficiency of the RNase treatment. In contrast, Ska1-TAP showed a sedimentation profile different from Ski3-TAP and Pab1-TAP. We observed an enrichment for Ska1 in the fractions mainly sedimenting around the 40S and 60S peaks but not within the 80S peak (Fig 1E).

These results indicated that following RNase treatment, Ska1 is still associated with large complexes but not with the 80S ribosome and the polysomes, suggesting that the weak association of Ska1-TAP to the ribosome is RNA-dependent. The presence of Ska1-TAP in several fractions of the gradient suggested that Ska1 could be associated with different complexes. Altogether, these results indicate that there are at least two different SKI complexes, one containing Ska1.

Ska1 is involved in the 3' to 5' degradation of mRNAs

Since Ska1 physically interacts with the SKI complex, we determined whether Ska1 participates in the same pathways as the SKI complex. The SKI complex contributes to the degradation of a number of RNA substrates, including normal mRNAs but also aberrant ones such as Non-Stop mRNAs. To test the effect of SKA1 removal on the general mRNA degradation pathway, we followed the behaviour of the well-characterised *PGK1pG* reporter gene

expressing a stable transcript (Anderson & Parker, 1998). The Stop codon is followed by a polyG tract which blocks the progression of Xrn1 in the 3'UTR allowing the detection of 3' to 5' degradation intermediates (Fig 2A; Anderson & Parker, 1998). With this *PGK1pG* reporter gene, the full-length mRNA is detected as well as a small 3'UTR fragment that accumulates as a result of the polyG blocking Xrn1. As previously observed (Anderson & Parker, 1998), the absence of Ski2 or Ski7 resulted in the accumulation of a short 3'UTR degradation intermediate, indicative of the inefficient 3' to 5' degradation in the absence of a functional SKI complex. Importantly, the absence of Ska1 resulted in the accumulation of the same 3'UTR intermediate fragment (Fig 2B). In contrast, the absence of Ska1 has no effect on the degradation of NSD targets (see below, Fig 2C). This result indicates that Ska1 is involved in the same general mRNA decay mechanism as the Ski factors concerning the 3'UTR regions.

If Ska1 is involved in the 3' to 5' degradation mRNA pathway, we postulated that the absence of Ska1 combined with mutation into genes involved in the 5'-3' mRNA degradation pathway should be deleterious for cells. Since the absence of the decapping enzyme Dcp2 severely affects cell growth, we used the Dcp2 degron fusion protein (*dcp2d* mutant) to induce its degradation in the presence of auxin (IAA). We combined this *dcp2d* mutant version with a *ski2Δ* or *ska1Δ* mutation. Growth of *ska1Δ* or *ski2Δ* mutant strains was not affected as compared to a *dcp2d* strain in the presence of auxin. In contrast, the double-mutant strains were sensitive to auxin (Fig 2D). We observed a synthetic lethality phenotype for cells combining *ski2Δ* and the *dcp2d* mutant, as previously described (Anderson & Parker, 1998). Although less severe, a *dcp2d ska1Δ* strain also showed a marked growth defect.

Ska1 is more specifically required for the degradation of long 3'UTR-containing RNAs

Since we observed intermediates of degradation accumulating in the absence of Ska1 or Ski2 using a *PGK1pG* reporter gene (Fig 2B), we analysed the genome-wide effect of *SKA1* removal. To detect any deficiency of the 3' to 5' RNA degradation pathway, we inactivated the major 5'-3' pathway. Upon *XRN1* deletion, mRNAs accumulate as decapped molecules, while the deletion of *DCP2* or *DCP1* severely impairs growth. In order to preserve more physiological conditions at the time of analysis, we used a *dcp2d* mutant, which strongly decreases mRNA decapping upon auxin addition, protecting mRNA 5'-ends from the Xrn1 exonucleolytic degradation. We mapped and quantified RNA 3'-ends genome-wide in a wild-type and in single- and double-mutant strains combining the *dcp2d* mutant with the *ska1Δ* or *ski2Δ* mutations. We used an anchored oligo-dT cDNA-priming step to generate 3'-end RNA sequencing libraries. Since the 3' to 5' RNA degradation intermediates are predicted to be devoid of polyA, we added an *in vitro* polyadenylation step using polyA polymerase. RNAs were extracted after 2 h of auxin treatment. Note that the vast majority of the Dcp2 protein was already depleted after 1 h of auxin treatment (Fig EV3A). However, we performed RNA analysis after 2 h of treatment in order to allow degradation intermediates to accumulate (see below). Examining the results with the Integrative Genomics Viewer (IGV; Robinson et al, 2011), one of the most striking phenotypes observed with the *dcp2d ski2Δ* double mutant, in comparison with the *dcp2d* single mutant, was an accumulation for

many mRNAs, of trimmed 3'-ends over a distance of about 50 nucleotides from the polyA sites (Figs 3A and B, and EV3B). These 3' trimmed transcripts were not visible in the *dcp2d* or *ski2Δ* single mutants. These shortened transcripts are likely 3' to 5' RNA degradation intermediates that accumulated over the Dcp2 depletion period (2 h in this experiment) when the 3' to 5' exonucleolytic activity of the exosome is very inefficient as a result of the SKI complex disruption in the *ski2Δ* mutant. Importantly, similar degradation intermediates were also observed in the *dcp2d ska1Δ* double mutant confirming that Ska1 is important for the 3' to 5' mRNA decay pathway, in agreement with the observation made with the *PGK1pG* reporter gene (Fig 2B). Although the deletion of either *SKA1* or *SKI2* in a *dcp2d* background showed similar effects on relatively long 3'UTRs (Figs 3A and EV3B), removal of Ska1 did not result in changes for many mRNAs with very short (less than ~60–70 nucleotides) 3'UTRs (Figs 3B and EV3B). Using Northern blot analysis upon RNase H digestion, we confirmed that the extent of 3'-end trimming was dependent on the duration of Dcp2 depletion (Fig EV3C; note that the *RPS31* gene belongs to the “short 3'UTR” category, not sensitive to Ska1). Thus, these shortened transcripts most likely correspond to 3' to 5' RNA degradation intermediates that accumulated following Dcp2 depletion.

We investigated the correlation between the length of the 3'UTR and the effect of Ska1 removal on the 3' to 5' degradation. To this end, we performed genome-wide analysis on total mRNAs and on mRNAs divided into three groups according to their 3'UTR lengths: genes with short 3'UTRs (16–60 nucleotides), genes with 3'UTRs of intermediate lengths (60–150 nucleotides) and genes with 3'UTRs longer than 150 nucleotides (Fig 3C and F, and Appendix Fig S1). To specifically analyse the degradation intermediates, we eliminated the normal cleavage and polyadenylation sites (i.e. the *bona fide* cleavage and polyA sites) as determined with the samples in which the *in vitro* polyadenylation step was omitted. Furthermore, to avoid the metagene signal being dominated by a few strongly expressed genes, the number of reads was normalised by the relative expression of the corresponding genes, as determined by standard RNAseq (see Materials and Methods). Figure 3F shows that long 3'UTRs share a similar profile of accumulation of 3' trimmed RNA intermediates in the absence of Ska1 or Ski2. In contrast, in the group of short 3'UTRs (less than 60 nucleotides), the degradation intermediates accumulated to a much lower extent in the absence of Ska1 when compared to the absence of Ski2 (Fig 3D). The group of genes with intermediate 3'UTR lengths exhibited an intermediate phenotype (Fig 3E). These observations were confirmed by analysing the probability (*P*-value) that the distribution of reads corresponding to *dcp2d ski2Δ* and *dcp2d ska1Δ* is the same at each position. No significant difference between the distributions of the 3'UTRs longer than 150 nucleotides (pink curve) was observed, while a very significant difference for the 3'UTRs shorter than 60 nucleotides was seen (green curve; Fig 3G and Appendix Fig S2). Altogether, these results showed that the absence of Ska1 or Ski2 leads to a similar 3' degradation for the long 3'UTRs. To analyse a set of transcripts with long 3'untranslated region, we examined lncRNAs such as the XUTs and the SUTs, which are cytoplasmic pervasive transcripts containing only short spurious ORFs and very long untranslated 3' regions. We aligned the reads of the XUTs or SUTs on their transcription termination sites (TTSs). In agreement with our

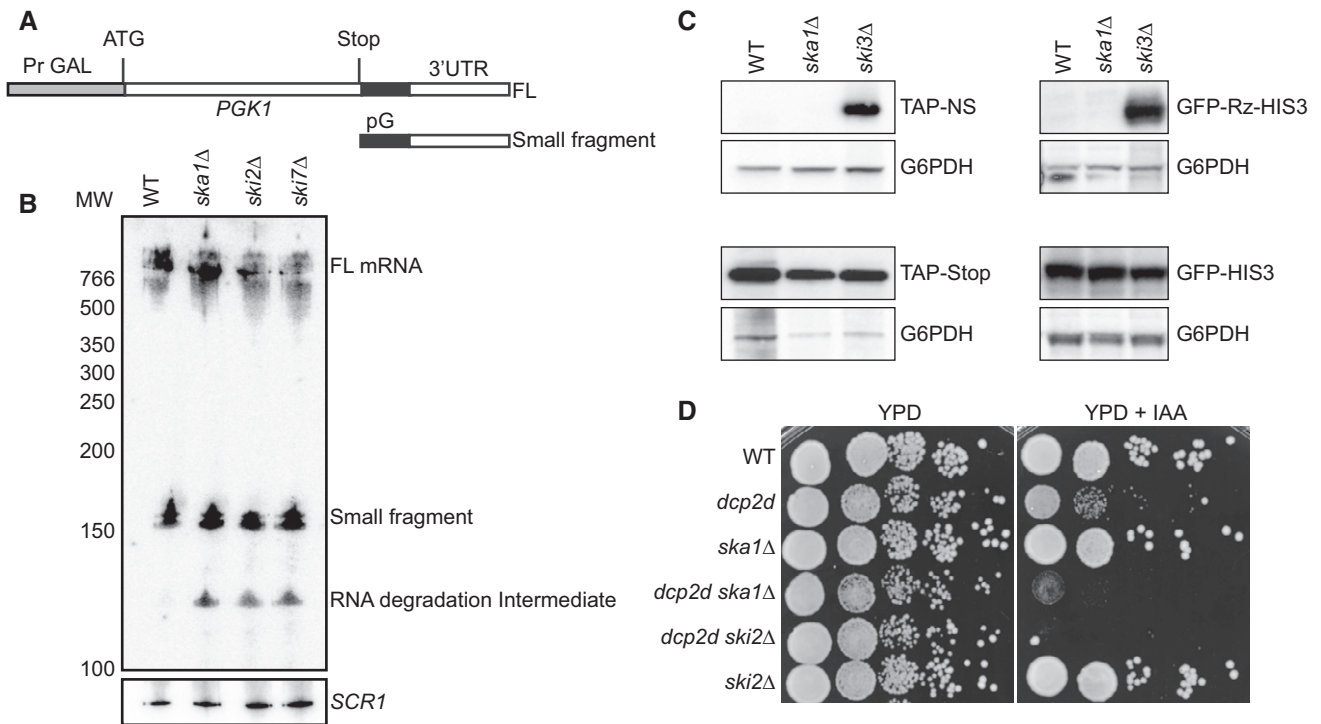


Figure 2. Ska1 is involved in the 3' to 5' mRNA degradation pathway.

- A Schematic representation of the *PGK1pG* reporter gene (Anderson & Parker, 1998). Top: the grey box represents the *GAL1* promoter region (PrGAL), the white boxes the *PGK1* transcribed sequences and the black box the polyG tract inserted just downstream of the *PGK1* Stop codon. Bottom: the 170 nucleotides fragment that accumulates as a result of the blockage of the 5'-3' exonucleolytic degradation by the polyG sequence.
- B Total RNA from wild-type, *ska1Δ*, *ski2Δ* and *ski7Δ* strains grown in presence of galactose was separated on a 6% polyacrylamide urea gel. Northern blot was performed with a [³²P]-polyG targeting probe. The membrane was then hybridised with a [³²P]-radiolabelled *SCR1* oligonucleotide as a loading control. MW, positions of the DNA fragments (in nucleotides) used as molecular weight ladder. FL, full length.
- C Ska1 is not required for Non-Stop mRNA degradation. Total cellular extracts were prepared from strains transformed with the reporter plasmids TAP-Non-Stop, GFP-Rz-HIS3, TAP-Stop or GFP-HIS3 were separated on a 10% SDS-PAGE polyacrylamide gel. Protein A and GFP were revealed by Western blot using a PAP antibody and an anti-GFP antibody, respectively. A loading control was obtained using an anti-G6PDH antibody.
- D *ska1Δ* is synthetic lethal with the *dcp2d* mutant. Serial dilutions of yeast strains, as indicated, were spotted on rich medium plates in the presence or absence of auxin (0.1 mM) and incubated for 48 h at 30°C.

Source data are available online for this figure.

hypothesis, we observed a similar profile of 3' trimming in the absence of Ska1 or Ski2 (Fig 3H). The observation that the deletion of *SKA1* or *SKI2* had similar effects on the accumulation of XUTs or SUTs was confirmed by an RNAseq approach (Fig 3I). We impaired the 5'-3' degradation pathway by depleting Dcp2 in strains lacking *SKA1* or *SKI2*. We clearly observed a similar accumulation of the XUTs and SUTs in these strains (Fig 3I). In contrast, mRNAs accumulated more in the absence of Ski2 than in the absence of Ska1 (Fig 3J). This observation is consistent with the synthetic lethal effect on the growth that we observed previously (Fig 2D). Using IGV, we focused on a specific XUT (5F-139) and verified its enrichment by Northern blot (Fig 4A and B, and Appendix Fig S3). This transcript accumulated upon depletion of Dcp2 and the effect was more marked when the depletion of Dcp2 was combined with a deletion of *SKI2* or *SKA1*. These results, showing that Ska1 is necessary for the degradation of the long 3'UTRs but not for the short ones, suggest that Ska1 could be specifically required with the SKI complex to target cytoplasmic RNA regions devoid of ribosomes.

Ska1 is not required for the degradation of NSD targets

We have previously shown that NSD substrates are associated with the ribosome at their 3'-ends (Schmidt *et al*, 2016). Therefore, we postulated that, in contrast to the SKI complex, Ska1 is not involved in the degradation of Non-Stop mRNAs. To test this hypothesis, we assessed the expression of the TAP-Non-Stop and the GFP-Rz-HIS3 reporter genes (Defenouillère *et al*, 2013; Kobayashi *et al*, 2010) in the presence or the absence of Ska1 (Fig 2C). Both reporters are sensitive to the NSD pathway. The TAP-Non-Stop reporter gene codes for Protein A, but lacks a Stop codon. The polyA tail is thus translated into a poly-lysine stretch, which, due to its high electrostatic charge, gets stuck at the ribosome exit tunnel, resulting in translation stalling. In contrast, the GFP-Rz-HIS3 reporter gene carries a ribozyme, which generates an mRNA coding for GFP without a Stop codon and a polyA tail. As a result, translation stops only when the ribosome reaches the very end of the transcript. We performed Western blot analyses with total cellular extracts from the *ska1Δ*, *ski3Δ*, wild-type strains transformed with plasmids

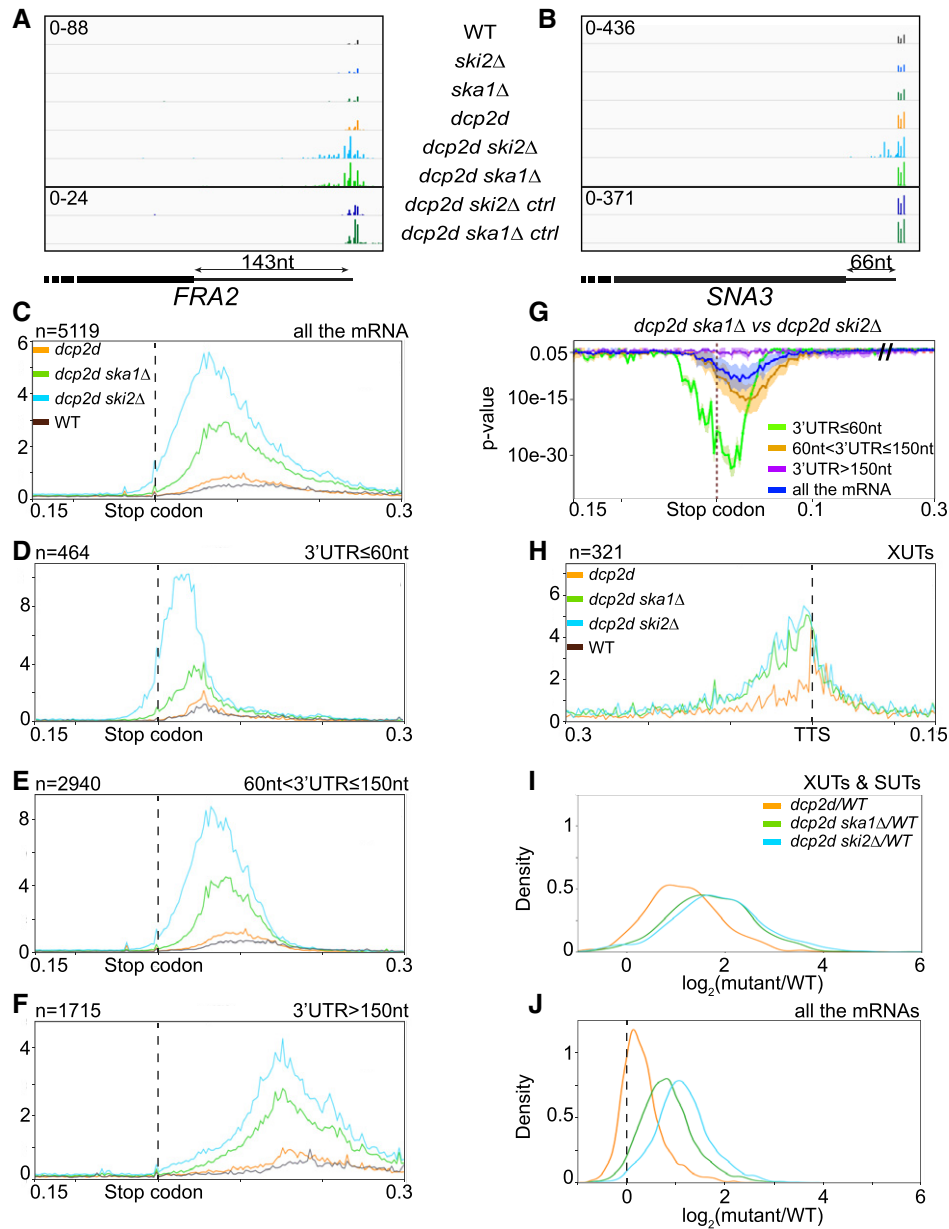


Figure 3. Ska1 and the SKI complex are required to degrade cytoplasmic RNA sequences devoid of ribosomes.

- A, B Visualisation of two loci, *FRA2* (long 3'UTR) and *SNA3* (short 3'UTR), using IGV to show the accumulation of 3'-end mRNA intermediates in the absence of the SKI complex or in the absence of Ska1 when the 5'-end degradation pathway is compromised. The name of the strains is indicated for each row, with "ctrl" standing for "control experiment without the *in vitro* polyadenylation step", allowing the visualisation of the naturally polyadenylated 3'-ends. The scheme at the bottom of the figure depicts the 3' part of the genes with the thick box representing the end of the ORF and the line the 3'UTR. The values on the y-axis represent the number of reads per position after autoscaling the various samples.
- C Genome-wide analysis of 3'-end mRNAs with protein-coding genes aligned on their Stop codons. The curves indicate the distribution of 5'-end read counts for each condition, computed for each position ranging from -150 to +300 nucleotides relative to the Stop codons (see Materials and Methods for more details). The distributions correspond to the average distributions of three independent replicates (see Appendix Fig S1 for the data from all single experiments).
- D-F As in (C) but for three groups of genes classified according to their 3'UTR length.
- G *P*-value distributions corresponding to the probabilities that the distribution of reads corresponding to *dcp2d ski2Δ* and *dcp2d ska1Δ* are the same at each position were computed by Mann-Whitney *U*-test function using *scipy.stats* v0.19.1. The *P*-value distributions (ribbon) joined with means (line) were computed on forty times resampling by taking randomly 400 genes into each gene set.
- H As in (C) but for XUTs aligned on the transcription termination sites (TTSs) and for positions -300 to +150 nucleotides relative to the TTS.
- I, J Frequency distributions of the ratios of RNAseq read counts for mutant mRNAs compared with wild type for mRNAs (J) and XUTs and SUTs (I), respectively. RNA libraries were constructed with the TruSeq stranded mRNA sequencing kit. mRNAs, XUTs and SUTs used for genome-wide analysis are listed in Dataset EV2.

expressing these reporters. As controls, we used the same reporter genes but with a normal termination codon or without a ribozyme. We did not observe any aberrant protein accumulation in the *ska1Δ* strain. In contrast, the *ski3Δ* strain positive control exhibited a strong accumulation of these aberrant polypeptides (Fig 2C). These results indicated that Ska1 is not involved in the Non-Stop aberrant mRNA degradation pathway.

This observation prompted us to determine whether natural premature polyadenylation sites, which have all the attributes of natural NSD substrates, and which are located within coding sequences, could be unaffected by the absence of Ska1. Such prematurely terminated transcripts have been described for genes such as *RNA14* and *AEP2* (Sparks & Dieckmann, 1998). We detected a strong accumulation of the corresponding transcripts in the absence of Ski2 but not in the absence of Ska1, both within the 3'-end RNAseq data, visualised using IGV, and Northern blots (Fig 4C–F and Appendix Fig S3C). Furthermore, these accumulated transcripts were already detected in the 3'-end RNAseq data without *in vitro* polyadenylation, demonstrating that they were polyadenylated *in vivo* (Fig 4C–F). Note that these transcripts accumulated to a much greater extent in the *dcp2d ski2Δ* double-mutant strain than in either the *dcp2d* or *ski2Δ* single mutants. This shows that the 5'-3' pathway can efficiently substitute to the 3' to 5' pathway when this later is absent.

The *HAC1* gene is of particular interest to discriminate between the effect of Ska1 on ribosome-associated and ribosome-free RNA 3'-ends. The *HAC1* transcript contains a peculiar intron, which is cleaved by a splicing endonuclease complex generating two cleavages, one at the end of exon 1 and one at the end of the intron (Sidrauski *et al*, 1996). The cleaved 3'-end of exon 1 is associated with a ribosome but not the intron sequence (Guydosh & Green, 2014). We observed that the absence of Ski2 impaired the degradation of both transcripts. In contrast, removing Ska1 did not lead to the accumulation of the exon 1 while it resulted in the accumulation of an exon 1–intron (Fig 4G and H, and Appendix Fig S3C), albeit to a lesser extent than in the absence of Ski2, as it is often observed for long 3'UTRs (Figs 3C and 5A).

In summary, Ska1 is clearly not required for the 3' to 5' degradation of NSD substrates, that are known to necessitate the association of the SKI complex to the terminal ribosome.

The ribosome density within the ORF influences the sensitivity of an mRNA to Ska1

Although our results strikingly showed that Ska1 was important for the degradation of mRNAs with long 3'UTRs, there are Ska1-sensitive mRNAs with short 3'UTRs (Fig 3D). We hypothesised that, in addition to the 3'UTR length, other parameters or features might determine the degree of sensitivity of mRNAs towards Ska1-dependent 3' to 5' degradation.

We observed that some genes within the short 3'UTR class carry uORFs. When uORFs are efficiently recognised by the translation machinery, it results in the main ORF being very poorly translated (Arribere & Gilbert, 2013). In such situation, the transcript effectively behaves as an RNA with a very short ORF followed by a very long 3'UTR, very much like XUTs or SUTs, for which Ska1 and Ski2 are equally important. Figure EV4A shows three uORFs-containing mRNAs with short 3'UTRs (considering the main ORF) and for

which Ska1 was as important as Ski2 for their efficient 3'-5' degradation.

We extended these observations by analysing, on a genome-wide scale, the relationship between the sensitivity to Ska1 and the translation level of mRNAs. To this end, it was necessary to determine, on a gene-to-gene basis, the relative degree of sensitivity of mRNAs towards Ska1 and Ski2. Using the 3'-end sequencing data, we determined on a gene-to-gene basis, the relative amount of intermediates accumulating in *dcp2d ska1Δ* versus *dcp2d ski2Δ* cells. A low ratio points to an mRNA insensitive to Ska1. Figure 5A plots, for each gene, the log₂ of this ratio against the lengths of the 3'UTRs. The link between Ska1 sensitivity and 3'UTR length was very well apparent in this representation and statistical analysis confirmed that the 3'UTR length is indeed an important feature determining the sensitivity of mRNAs towards Ska1 (panel inside Fig 5A). Yet, one also sees that, for short to medium size 3'UTR-containing mRNAs, the sensitivity towards Ska1 relative to Ski2 was very variable.

We found that a large part of this variability could be explained by differences in ribosome density within the ORFs, which largely correlates with translation efficiencies (Ingolia *et al*, 2009). mRNAs with short 3'UTRs were much less sensitive to Ska1 when they were robustly translated (20% highest ribosome densities) than when poorly translated (20% lowest ribosome densities; Fig 5B). The correlation between Ska1 insensitivity and ribosome density within the ORF could also be observed for medium size (100–200 nt) 3'UTR-containing mRNAs, although to a lesser extent compared to short (< 100 nt) 3'UTR-containing mRNA (Fig 5C, middle and left panel, respectively). In contrast, long (> 200 nt) 3'UTR-containing mRNAs were not significantly affected by ribosome density within the ORF (Fig 5C, right panel). We verified that there was no correlation between the 3'UTR length and the translation efficiency (Appendix Fig S4). In summary, our results show that, in addition to the length of the 3'UTR, which remains the primary determinant of Ska1 sensitivity, the translation efficiency is an important feature that affects the sensitivity of an mRNA towards Ska1.

The length of the 3'UTR directly affects the sensitivity of an mRNA towards Ska1

The observations reported above identified the 3'UTR length as a prominent feature that determines the involvement of Ska1 in targeting an mRNA for 3' to 5' degradation. To directly test the influence of the 3'UTR length, we decided to analyse whether lengthening the 3'UTR of a gene could turn it from being insensitive to being sensitive to Ska1. To do so, we first introduced these modifications seamlessly in the chromosomal copy of a gene. In order to be able to monitor the accumulation of 3' degradation intermediates from the chromosomal copy of this gene, it had to be well expressed. We selected *TDH3*, which is strongly expressed, carries a relatively small 3'UTR (98 nt for the shortest isoform; Fig 6A) and is well translated. In accordance, degradation intermediates strongly accumulate upon auxin addition in the *dcp2d ski2Δ* strain but not in the *dcp2d ska1Δ* strain (Figs 6A and B, *TDH3* WT; and EV5A). We introduced two different types of sequences directly after the ORF Stop codon; a 110-nucleotide long sequence derived from the 3'UTR of the *Schizosaccharomyces pombe* *PYK1* gene or a 205-nucleotide long sequence derived from the ORF of the same

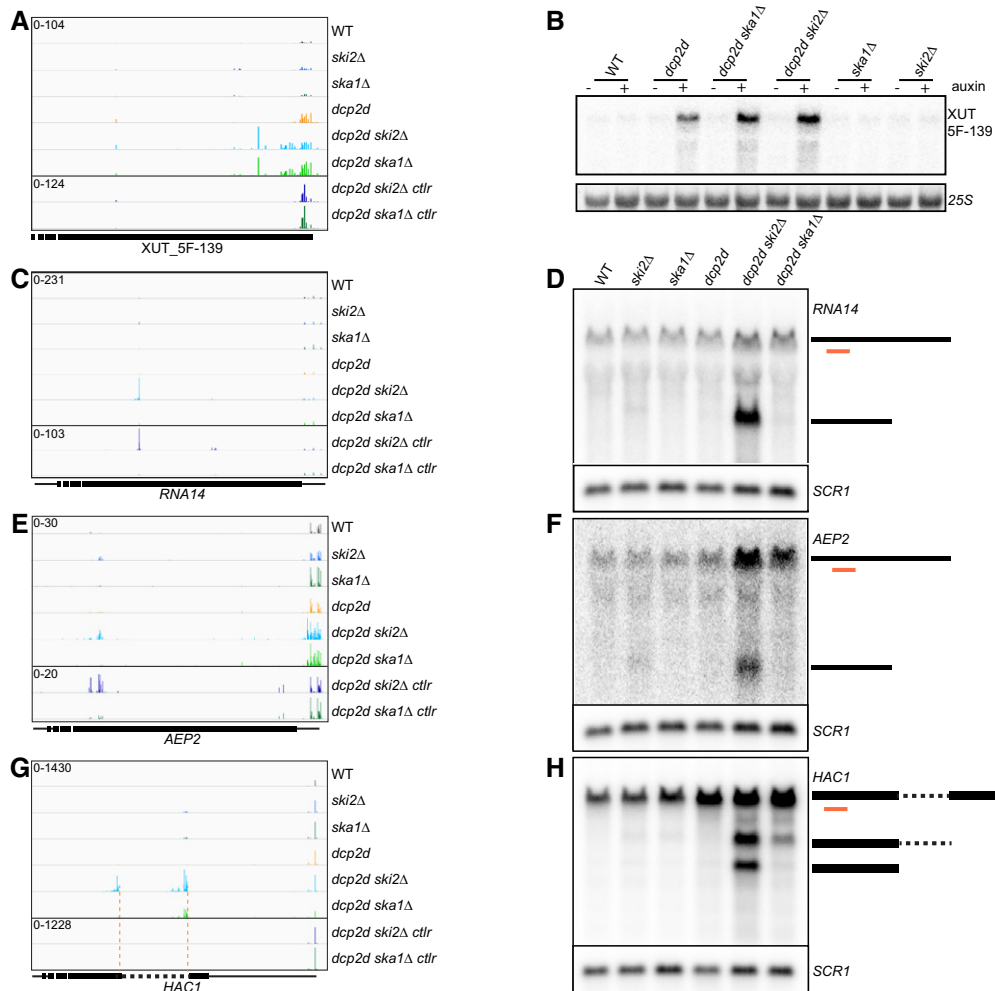


Figure 4. Ska1 is required for the degradation of XUTs but not of NSD targets.

- A Visualisation of the *XUT_5F-139* locus using IGV. Rows labelled as in Fig 3. The number of reads per position is indicated as in Fig 3.
- B The Northern blot was performed with total RNAs from yeast strains treated or not with auxin for 2 h. RNAs were separated, after denaturation at 65°C in formazol, on a 1% agarose gel and the blot hybridised with a [³²P]-radiolabelled *XUT_5F-139* RNA probe and then with a [³²P]-radiolabelled 25S rRNA oligonucleotide probe as a loading control.
- C, D Visualisation of the *RNA14* locus using IGV. The different forms of the mRNA are schematised on the right by black lines, with the position of the RNA probe in orange. A [³²P]-radiolabelled *SCR1* oligonucleotide probe was used as a loading control.
- E, F As in (C, D) but for the *AEP2* transcript.
- G Visualisation of the *HAC1* locus in the different strains using IGV. The orange dotted lines indicate the splicing sites.
- H As in (D, F) but for the *HAC1* transcripts. The dotted and thick black lines on the right schematise the intron and exon sequences, respectively.

Source data are available online for this figure.

gene. This resulted in the lengthening of the *TDH3* 3'UTR from 98 nt to 208 and 303 nt, respectively (*TDH3-208* and *TDH3-303* in Fig 6A). These insertions rendered the *TDH3* mRNA sensitive to Ska1 in a very similar manner in both *tdh3* mutant strains (Figs 6B and EV5A). Note that degradation intermediates accumulated upon auxin addition to lengths very similar in the *dcp2Δ ska1Δ* and *dcp2Δ ski2Δ* but not to the same level, in agreement with the general behaviour of long 3'UTR-containing mRNAs (Fig 3F). Conversely, we tested if shortening a long 3'UTR would result in insensitivity to Ska1. We chose to mutate *PGK1* because it carries a relatively long 3'UTR (158 nt) and we had previously shown that

the *PGK1pG* reporter is Ska1-sensitive (Fig 2B). We first confirmed that, even without the poly(G) sequence, *PGK1*, expressed from a plasmid (Fig 6C, left panel) showed, upon Dcp2 depletion, the same 3' degradation intermediate accumulation in *ska1Δ* and *ski2Δ* strains ("*PGK1* long 3'" in Fig 6D, left panel). After shortening the 3'UTR to 76 nt, the mRNA became largely insensitive to Ska1 ("*PGK1* short 3'" in Fig 6C and D, left panel and EV5B, left panel). We then introduced a premature Stop codon (PTC) into the *PGK1* ORF of these two distinct reporter genes to lengthen the actual 3'UTR without introducing major changes in the sequence (Fig 6C, right panel). This alteration made the *PGK1* mRNA sensitive to

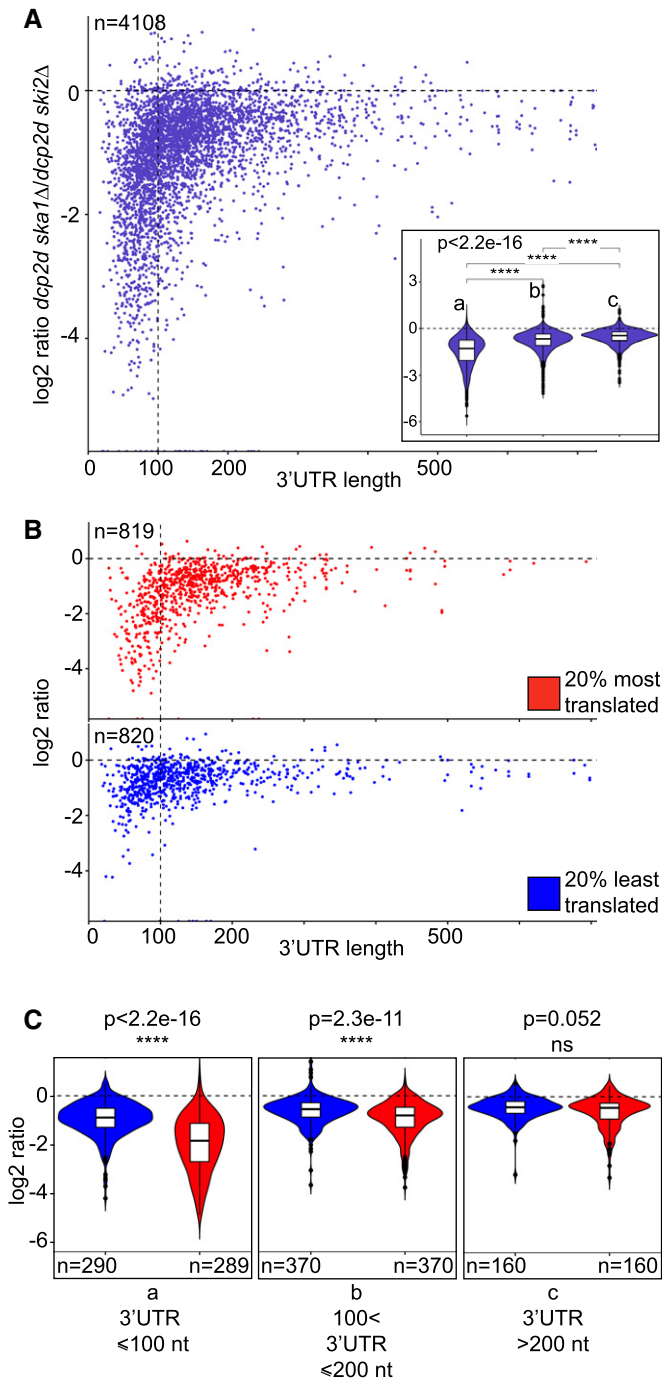


Figure 5. Translation efficiency is involved in Ska1-dependent 3' to 5' RNA degradation.

A A scatterplot between the log₂ mean ratio *dcp2d ska1Δ/dcp2d ski2Δ* and the 3'UTR length. The ratios were computed on clusters of 3' degradation intermediates determined using the coverage values of *in vitro* polyadenylated samples subtracted of the naturally polyadenylated 3'-ends. We discarded clusters associated to ORFs with low mRNA expression (see Appendix Supplementary Methods for details). The clusters of degradation intermediates are listed in Dataset EV3 (Inset). The genes were separated into three classes of 3'UTR size (a: 3'UTR ≤ 100 nt, n = 1,452; b: 100 < 3'UTR ≤ 200 nt, n = 1,850; c: 3'UTR > 200 nt, n = 806). The distribution of 3' degradation intermediate ratios is presented by violin plots with boxplots inside (showing the distribution's probability density), computed using ggpubr v0.1.8 package. Significant differences (Kruskal–Wallis P-value < 2.2e-16) were found for the ratio distributions between each size classes.

B 3' degradation intermediate clusters were classified according to the translation level of their corresponding mRNAs using the ribosomal density data from Ingolia *et al* (2009) (see Appendix Supplementary Methods for details). The two superposed panels represent scatter plots as in (A) for the 20% most (top; red dots) and 20% least (bottom; blue dots) translated mRNAs.

C Violin representations with boxplots inside (i.e. kernel density plot) and Wilcoxon statistical tests comparing the log₂ ratios, separated into three size classes as in (A, inset) and distinguishing the 20% most (red) and 20% least (blue) translated mRNAs as defined in B.

SKA1 overexpression affects the association of the SKI complex with the ribosome

All our results point to the existence of two distinct SKI complexes: one containing Ska1 that more specifically targets RNA 3'-ends in a ribosome-independent manner and one lacking Ska1, which directly associates with the ribosome. In one model, Ska1 would acts as a specific competitor of the SKI–ribosome interacting surface, preventing a fraction of the SKI complex from interacting with the ribosomes and keeping it available to directly target ribosome-free RNA 3'-ends. According to this model, overexpression of SKA1 should prevent SKI complexes from interacting with ribosomes, which should specifically affect the NSD degradation pathway (see above) but not the degradation of ribosome-free RNA regions.

To test the potential competition between Ska1 and ribosomes for the activation of the SKI complex, we investigated the effects of SKA1 overexpression on RNA degradation. In the NSD assay, SKA1 overexpression resulted in a strong accumulation of the Non-Stop ProtA (TAP-NS; Fig 7A). Note that the TAP-NS reporter gene is carried on a 2μ plasmid and we observed a weak heterogeneity of the TAP-NS expression due to the variation of the copy number present in the cells (Appendix Fig S5A). Therefore, to avoid this heterogeneity, we performed the experiment with a pool of transformants (Fig 7A). In contrast to its effect on the TAP-NS reporter, overexpressed SKA1 had no effect on the degradation of XUTs in *dcp2d ski2Δ* strain (Fig 7B and Appendix Fig S5B); yet, it was able to complement a SKA1 deletion, showing that it did not impair the function of the SKI complex for the degradation of ribosome-free RNA sequences. Similarly, we postulated that SKA1 overexpression should promote the formation of the small complex visualised in a sucrose gradient to the detriment of the SKI/80S particle. To test this hypothesis, we examined the sedimentation of Ski3-TAP in a sucrose gradient when SKA1 is overexpressed. In agreement with

NMD as shown by a reduced signal in WT cells (Fig 6D, right panel) and, as expected, transcripts were stabilised in Dcp2-depleted cells. Thus, the introduction of a PTC in *PGK1* resulted in the accumulation of 3' degradation intermediates with strains carrying the *dcp2d* gene in combination with deletions of *SKA1* or *SKI2*, an effect independent of the initial length of the 3'UTR (Fig 6D, right panel and EV5B, right panel).

These two independent experiments confirmed that the length of the 3'UTR is a key feature that distinguishes Ska1-sensitive from the Ska1-insensitive mRNAs.

our hypothesis, we observed that the Ski3-TAP sedimentation profile shifts from the 80S to the region where Ska1-TAP normally sediments (Fig 7C), *i.e.* lighter fractions around the 40S peak (see Fig 1D). These results are fully consistent with a model where Ska1 antagonises the formation of ribosome-SKI complexes, which are involved in the NSD pathway as well as the degradation of translated RNA sequences (Schmidt *et al*, 2016).

Discussion

Ska1 is a novel factor associated with a subpopulation of the SKI complex

Using affinity purification followed by quantitative mass spectrometry analyses, we identified a new component, Ska1, specifically associated with the SKI complex (Fig 1). The mass spectrometry analyses also revealed that, while the amount of Ska1 was about five to ten fold lower than the SKI complex in the Ski3-TAP purified complex, it was present in similar amounts to the SKI complex when Ska1-TAP was used as a bait for the affinity purification (Fig EV2). This strongly suggested that Ska1 is only associated with a fraction of the SKI complexes, defining Ska1-SKI as a new SKI subcomplex. While most of the SKI complex sedimented in a sucrose gradient in the 80S and the polysomal fractions, the Ska1-SKI complex mainly sedimented in lighter fractions (Fig 1D), which suggested that it is functionally distinct from the main SKI complex.

The Ska1-SKI complex is involved in the 3' to 5' RNA degradation pathway

The hypothesis that the function of Ska1 was related to the mRNA 3' to 5' degradation pathway was first strengthened by the fact that deletion of *SKA1* results in a synthetic growth defect when combined with the depletion of Dcp2, which is involved in mRNA decapping, one of the early steps of the 5'-3' mRNA degradation pathway (Fig 2D). One hypothesis could have been that Ska1 was involved in the assembly of the SKI complex. However, this possibility was not consistent with the fact that removal of Ska1 had no effect on the activity of the SKI complex on substrates of the Non-Stop decay pathway such as a Non-Stop reporters (Fig 2C) or mRNAs prematurely cleaved and polyadenylated within their ORFs (Fig 4C–H and Appendix Fig S3C).

The observation that the exosome is enriched in the Ska1-TAP affinity purification to an extent similar to its enrichment in the Ski3-TAP purification also suggested that Ska1 is directly involved in the 3' to 5' degradation pathway by assisting the exosome. We then hypothesised that the Ska1-SKI subcomplex might be involved in the degradation of a subset of the SKI substrates. The SKI complex is not only involved in the general mRNA degradation pathway as well as in aberrant mRNA degradation pathways such as the NSD or the NGD (Anderson & Parker, 1998; van Hoof *et al*, 2002; Doma & Parker, 2006; Tsuboi *et al*, 2012). While the absence of Ska1 did not affect Non-Stop substrates, it induced the accumulation of 3' to 5' degradation intermediates of the *PGK1pG* reporter in a manner very similar to the deletion of *SKI2* (Fig 2), supporting the hypothesis that the Ska1-SKI complex is involved in the degradation of only a subset of the SKI substrates.

In order to more precisely define which types of transcripts require the Ska1-SKI complex for their efficient 3' to 5' degradation, we performed a genome-wide analysis of the accumulation of 3' degradation intermediates in the absence of Ska1 or Ski2, in the context of a depletion of Dcp2 to abrogate the 5'-3' degradation pathway. It revealed that the Ska1-SKI complex is mainly involved in the degradation of mRNAs with relatively long 3' UTRs as well as cytoplasmic long non-coding RNAs (XUTs and SUTs; Figs 3, 4A and B, 5A, and EV3–EV5).

The Ska1-SKI complex assists the cytoplasmic exosome in the absence of a direct association with the ribosome

It has been known for a long time that the SKI complex operates in the cytoplasm as an exosome co-factor to degrade RNAs from their 3' ends. Recent findings show that the SKI-exosome complex functions co-translationally and the cryo-EM structure of the ribosome-SKI complex suggests that the helicase activity of Ski2 is activated by its direct association with the ribosome (Schmidt *et al*, 2016). This finding created a paradox because it is at odds with previous observations showing that the SKI complex is required for the efficient 3' to 5' degradation of mRNA 3'UTRs, which are RNA regions mostly devoid of ribosomes (Anderson & Parker, 1998). We hypothesised that the main function of the Ska1-SKI complex was to assist the cytoplasmic exosome in the absence of a direct interaction of the SKI complex with the ribosome. A series of observations supported this hypothesis.

When associated with the exosome (Fig 1C), Ska1 is not stably bound to ribosomes. The sedimentation of a small fraction of Ska1-TAP with the 80S fraction in a sucrose gradient is RNase-sensitive, suggesting that it might associate with ribosomes only indirectly, by the intermediate of mRNAs (Fig 1D and E). The sensitivity of mRNAs towards Ska1 is defined, for a large part, by the size of their 3'UTR (Figs 3, 5 and EV3, and Appendix Figs S1 and S2). One could argue that long 3'UTRs might carry co-evolved features that are specifically required for the recruitment of the Ska1-SKI complex. We ruled out this possibility by showing that lengthening with different types of sequences or shortening the 3'UTRs of reporter genes turned them from being insensitive to sensitive to Ska1 and *vice versa* (Figs 6 and EV5). Moreover, a short 3'UTR mRNA became equally sensitive to Ska1 and Ski2 upon introduction of a premature Stop codon, which effectively lengthened the 3'UTR without changing its distal sequence (Figs 6C and D, and EV5). This definitively showed that the distance between the 3'-end of a transcript and the ORF Stop codon is the primary determinant of the sensitivity towards Ska1. However, this was only true for well-translated mRNAs. The SKI complex seems to require Ska1 to efficiently assist the exosome on short 3'UTR-containing mRNAs if these are poorly translated (Fig 5B and C).

All these observations point to the determinant of Ska1 sensitivity being the absence of ribosomes at the proximity of the 3'-end of the transcript. Thus, during the 3' to 5' degradation of most mRNA sequences, which mainly consist of translated ORFs, the SKI complex could directly associate with the ribosome and assist the cytoplasmic exosome in the absence of Ska1 (Schmidt *et al*, 2016). However, Ska1 would be required when no ribosomes are sufficiently close to the SKI-exosome degrading complex at the end of the transcript. This suggests a model in which the general 3' to 5'

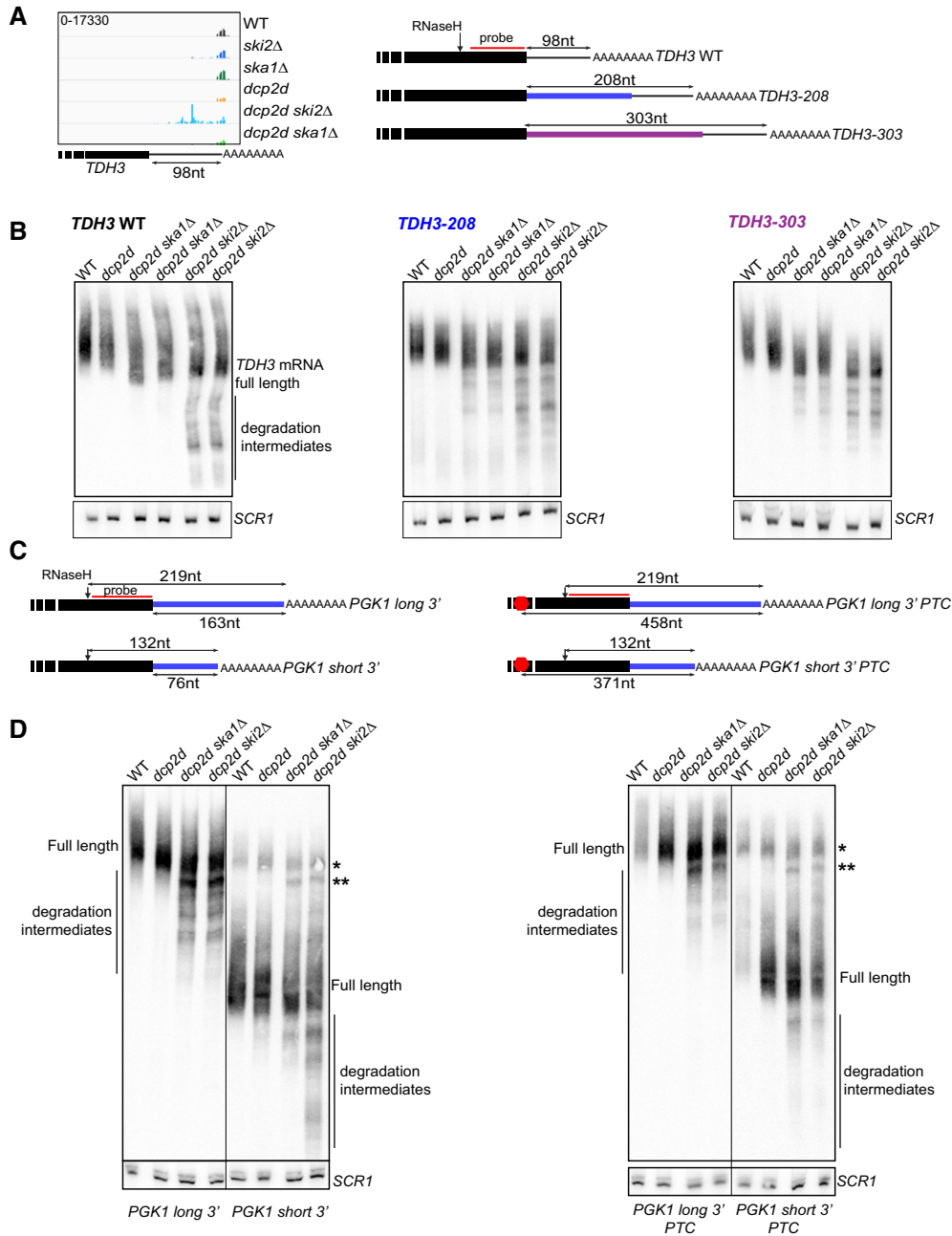


Figure 6. The length of a 3'UTR directly influences the sensitivity of an mRNA towards Ska1.

A Visualisation of the *TDH3* RNA 3'-end termini in the wild-type and mutant strains using IGV, as in Fig 3A (left panel). Schematics of the WT and *tdh3* mutant constructs (right panel). The black rectangles symbolise the end of the ORF, while the black line symbolises the 3'UTR. The thick blue and purple lines represent the sequences derived from the 3'UTR or ORF of the *Schizosaccharomyces pombe* *PGK1* gene, respectively. The vertical arrow symbolises the RNase H cleavage site. The red line schematises the RNA probe.

B Northern blots analysing the degradation intermediates of, respectively, the *TDH3*, *TDH3-208* and *TDH3-303* RNAs extracted from the cells treated for 2 h with 0.1 mM auxin and digested with RNase H in the presence of oligonucleotide AJ576. RNAs were separated on a 5% polyacrylamide urea gel and hybridised with the Digoxigenin-containing *TDH3* RNA probe. A [³²P]-labelled oligonucleotide hybridising to *SCR1* was used to provide a loading control.

C Schematic of *PGK1* reporter constructs. The black rectangles symbolise the end of the ORF, while the thick blue line represents the 3'UTRs. The red hexagon represents an artificial premature Stop codon. The vertical arrows symbolise the RNase H cleavage site. The red line schematises the Digoxigenin-containing RNA probe as in (A).

D Northern blot analysing the degradation intermediates of the *PGK1* reporter constructs, as in (B), after digestion with RNase H in the presence of oligonucleotide EsD52. Note that the background bands visible at the top of the *PGK1 short 3'* and *short 3' PTC* (indicated by * and **) correspond to the endogenous *PGK1* full 3'-end and first degradation intermediates, which are recognised by the oligonucleotide for the RNase H treatment and by the RNA probe. [³²P]-labelled oligonucleotide hybridising to *SCR1* was used to provide a loading control.

Source data are available online for this figure.

mRNA degradation pathway could act in two steps after deadenylation (Fig 8). First, a Ska1-associated SKI complex would assist the exosome to degrade ribosome-free RNAs, such as 3'UTR mRNA regions, until it became sufficiently close to the coding regions where it would encounter ribosomes. At this point, there are at least two models: Ska1 could dissociate from the SKI-exosome complex, allowing it to directly interact with the ribosome while remaining on the RNA being degraded (Fig 8). Alternatively, the Ska1-SKI-exosome could be exchanged for a "Ska1-free" SKI-exosome complex, which could directly interact with the ribosome. For non-translated RNA sequences, only the Ska1-SKI complex would assist the exosome, independently of the ribosome.

The question arises as to know at what point the switch from the Ska1-SKI complex to the ribosome-SKI complex occurs. Although no definite switch point could be identified in the metagene analysis (Fig 3C), the analysis of the 3' end sequencing data for mRNAs with intermediate 3'UTR lengths (between ~70 and 100 nucleotides; Fig EV4B) revealed similar profiles of 3'-degradation intermediates for the *dcp2d ski2Δ* and *dcp2d ska1Δ* mutants until a distance of 55–67 nucleotides away from the Stop codon (distances measured from the first nucleotide after the Stop codon), from which Ska1 was no longer required (no accumulation of degradation intermediates), while Ski2 was. Interestingly, if one estimates the length of the RNA expected to be protected by the ribosome-SKI-exosome complex, one finds similar figures. More specifically, the ribosome on the termination codon has been shown to protect about 12 nucleotides following the Stop codon (18 nucleotides when counting from the first nucleotide in the P site; Archer *et al*, 2016). Adding the length of the RNA fragment protected *in vitro* by the SKI complex (9–10 nucleotides; Halbach *et al*, 2013) and by the exosome (31–33 nucleotides; Malet *et al*, 2010) gives an expected range of protection between 52 and 55 nucleotides, counting from the first nucleotide following the Stop codon. This length range, when compared to the 55–67 nucleotides distance from the Stop codon from which Ska1 becomes dispensable (Fig EV4B) suggests that Ska1 is no longer required as soon as the SKI complex, which progresses from 3' to 5' along with the processive exosome (Dziembowski *et al*, 2007), comes sufficiently close to the last ribosome sitting on the Stop codon to directly interact with it.

What could be the precise molecular function of Ska1?

The data presented in this work strongly suggest that Ska1 is required for the SKI complex to assist the exosome in the absence of a direct interaction with a ribosome. However, the precise molecular function of Ska1 within the Ska1-SKI-exosome complex remains unknown. Ska1 is a highly basic (pI: 9.65) protein of 32.3 kDa. Although homologs can be found in other *Saccharomyces* species (SGD projet; <https://www.yeastgenome.org/cache/fungi/YKL023W.html>), Ska1 does not harbour any known protein domain and is therefore unlikely to have an enzymatic activity. Moreover, even for Ska1-sensitive mRNAs, the absence of Ska1 did not show an effect as strong as the absence of Ski2, suggesting that, in the absence of Ska1, the SKI complex could retain some ability to target mRNA 3' ends even in the absence of nearby ribosomes.

Several lines of evidence strongly suggest that the interaction of Ska1 with the SKI complex inhibits the interaction of the later

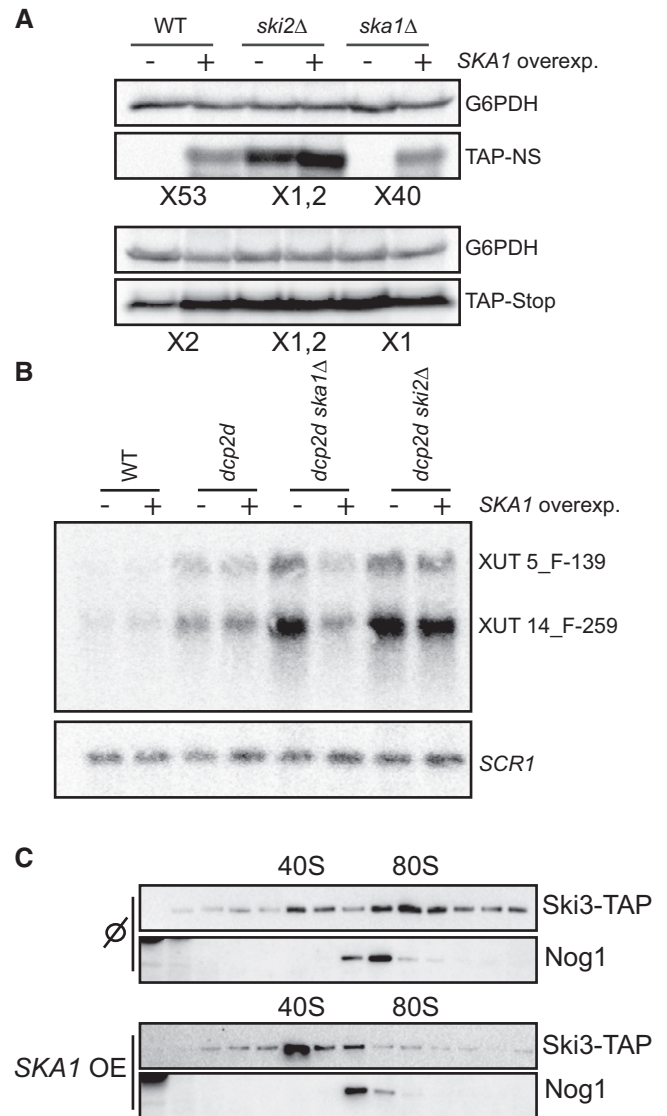


Figure 7. SKA1 overexpression affects Non-Stop mRNA decay.

A Total cellular extracts from a pool of clones transformed with the TAP-Non-Stop or the TAP-Stop reporter genes in addition to the pCM190 or the pCM190-SKA1 plasmids were separated on a 10% SDS-PAGE polyacrylamide gel. Protein A was revealed by Western blot using a PAP antibody. A loading control was done using anti-G6PDH antibody. Quantification of the TAP-Stop, TAP-NS and G6PDH bands was done with ImageJ software. First, the intensity of each TAP-Stop and TAP-NS band was normalised to the intensity of the corresponding G6PDH signal. Second, the ratio between the SKA1 overexpression and the empty vector was calculated and indicated below each blot.

B Northern blot with total RNAs from strains transformed with the empty vector pCM190 or the pCM190-SKA1 plasmid ("SKA1 overexp.") and treated with auxin for 2 h, hybridised with probes for XUTs 14_F-259 and 5_F-139. A SCR1-specific [³²P]-radiolabelled oligonucleotide was used as a loading control.

C Total cellular extracts from cells expressing Ski3-TAP and transformed with the empty pCM190 vector (∅) or with pCM190-SKA1 vector (SKA1 OE) were separated on a sucrose gradient (10–50%) by ultracentrifugation. Each fraction was analysed by Western blot using PAP for the detection of the TAP fusion proteins, as indicated. An anti-Nog1 antibody was used to mark the 60S fractions.

Source data are available online for this figure.

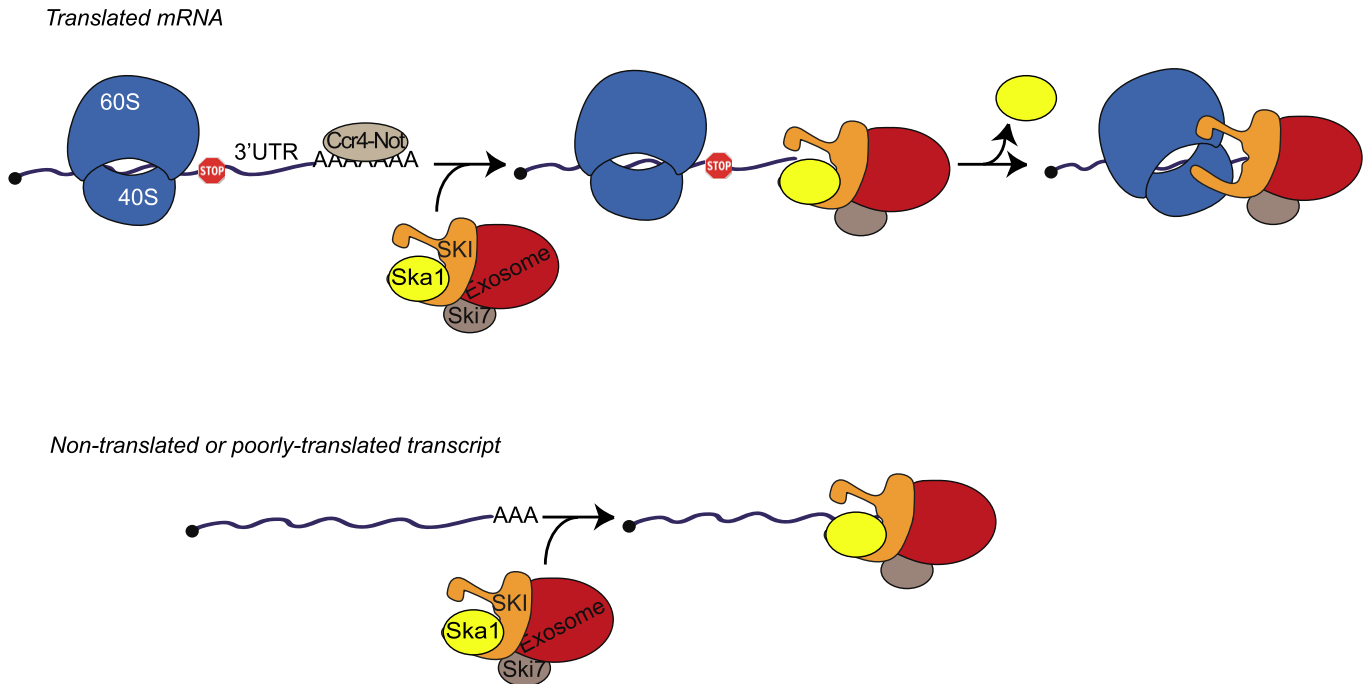


Figure 8. Model for SKI-ribosome and ribosome-independent SKI complexes functions.

For translated mRNAs (top), the Ska1-SKI complex would, in a first step, assist the exosome independently of the ribosome to degrade the 3'UTR; in a second step, when the SKI/Ska1 complex gets close to the coding sequence, there is an exchange between Ska1 and the ribosome for its association with the SKI complex. The degradation of a non-translated or poorly translated transcript could occur entirely independently of the ribosome (bottom).

with the ribosome. First, the overexpression of *SKA1* inhibits the degradation of an NSD substrate, known to involve the SKI-ribosome interacting complex, while it did not affect the 3' to 5' degradation of XUTs (Fig 7A and B). The interaction of the SKI complex with ribosomes results in the SKI complex sedimenting, in a wild-type strain, in the 80S and polysome fractions of a sucrose gradient (Schmidt *et al.*, 2016). The overexpression of *SKA1* strikingly modifies this sedimentation profile, the SKI complex (identified by Ski3-TAP) being displaced from the 80S and polysome fractions to much lighter fractions of the gradient (Fig 7C), where Ska1 can be found (Fig 1D). These observations strongly suggest that the interaction of Ska1 with the SKI complex precludes the interaction of SKI with the ribosome. The SKI complex has been shown to have a strong affinity for ribosomes carrying 3' RNA overhangs that are likely to be abundant in cells and thus susceptible to sequester most SKI complexes (Schmidt *et al.*, 2016). Since we found that the interaction of the SKI complex with Ska1 was antagonistic with its interaction with the ribosome (Fig 7), a possibility would be that a major role of Ska1 is to prevent a fraction of the SKI complex from interacting with ribosomes, making it available for assisting the degradation of ribosome-free RNA sequences. According to this hypothesis, the only function of Ska1 would be to act as an antagonist of the SKI-ribosome interaction. Yet, the determination of the structure of the SKI-ribosome complex showed that the interaction between Ski2 and the 40S is important to activate the Ski2 helicase (Schmidt *et al.*, 2016). This raises the possibility that Ska1 would play a similar role when it interacts with the SKI complex. Further experiments will be required to test this hypothesis.

Materials and Methods

Yeast strains and plasmids

Yeast strains and plasmids used in this study are listed in Appendix Tables S1 and S2, respectively. The yeast strains generated for this study were obtained by transformation of genomic PCR products. Details of constructions are in Appendix Supplementary Methods.

Polysome gradients, protein extraction and Western blotting

Polysome extracts and sucrose gradients were performed as described (Defenouillère *et al.*, 2013). Total protein extracts were obtained by alkaline treatment using 5 A_{600} mid-log phase yeast cells. The extracts were separated on 10% SDS-PAGE polyacrylamide gel. The proteins were transferred on nitrocellulose membrane using a Bio-Rad semi-dry machine. The membrane was hybridised with appropriate antibody dilutions (see Appendix Table S3).

RNA extraction and Northern blot analysis

Total RNA was purified from 12 A_{600} mid-log phase yeast cells using the hot acid phenol protocol (Collart & Oliviero, 2001). RNAs were separated on 1% agarose gel, transferred on nylon membranes (Hybond N⁺, Amersham) and probed with ³²P-labelled oligonucleotides or with ³²P-labelled RNA probe synthesised according to the Ambion MAXIscrip[®] Kit procedure using

the oligonucleotides listed in Appendix Table S4. As indicated in the legends, some RNAs were revealed using Digoxigenin-containing RNA probes. These were generated by *in vitro* transcription with T7 polymerase using the DIG RNA Labelling kit (SP6/T7) from Roche (cat. No 11175025910). The oligonucleotide AJ529 (T7 promoter) pre-annealed with a target-specific oligonucleotide composed of the T7 promoter reverse complement fused to a template sequence (see Appendix Table S4) were used as a template. For *PGK1* constructs, the RNA probe was generated from EsD53 oligonucleotide and it is complementary to the end of the *PGK1* ORF and the beginning of 3'UTR (from nucleotide -56 to the nucleotide +15 situated just before the inserted SpeI site). For *TDH3* mRNA, the RNA probe was generated by *in vitro* transcription after annealing of AJ529 with AJ575.

Library constructions

Three independent biological replicates were generated for wild-type, single- and double-mutant strains. Cells were grown to exponential phase and treated with auxin (final concentration 0.1 mM) for 2 h. Reference aliquots of *S. pombe* were added and total RNA isolated. Five microgram of total RNA was treated with Turbo DNaseI for 20 min at 37°C. After phenol/chloroform extraction, RNAs were precipitated with ethanol and resuspended in water. A depletion of the ribosomal RNA was performed using Ribo-Zero Gold rRNA removal kit for yeasts (Illumina). Removal of the rRNA was verified using a Bioanalyzer. An *in vitro* polyadenylation was performed with 4 units of PAP in the presence of 50 µM cordycepin and 1 mM ATP. After phenol/chloroform extraction, RNAs were precipitated with ethanol and resuspended in water. The 3'mRNA-Seq libraries were constructed using the Lexogen QuantSeq 3'mRNA-Seq Library Prep Kit for Illumina (Rev) with Custom Sequencing Primer according to manufacturer's instructions. The RNAseq libraries were made using 5 µg of total RNA treated with Turbo DNase and Ribo-Zero as described above. The libraries were constructed using TruSeq stranded mRNA LT sample prep Kits (Illumina) according to the manufacturer's instructions. Since the mutants of interest are involved in the classical mRNA degradation pathway, we added *Schizosaccharomyces pombe* (*S. pombe*) cells to the *S. cerevisiae* cell pellet for spiked-in normalisation. The total read counts for each library are indicated in Appendix Table S5. The reproducibility of the 3'mRNA-Seq and RNAseq libraries experiments, respectively, was tested by Spearman correlation (Appendix Fig S6A) and Principal Component Analysis (PCA; Appendix Fig S6B) for three independent biological replicates per strain. The replicates for each mutant strain clustered together and aside from the other strains.

Bioinformatics analyses

Bioinformatics analyses are described in the Appendix Supplementary Methods.

The sequencing data are available from European Nucleotide Archive (accession number for all TTS sequencing samples under the accession codes ERS2548668 to ERS2548690 and for all RNA sequencing samples under the accession codes ERS2548828 to ERS2548845).

Affinity purifications coupled to mass spectrometry

Affinity purifications were performed using 4 l of culture at 2 A₆₀₀ as described in Defenouillère *et al* (2013). Briefly, proteins were digested in solution, and then, peptides were analysed using an LTQ-Orbitrap Velos. Protein identification and comparative label-free quantification were performed using the MaxQuant suite (version 1.5.5.1) and the embedded Andromeda search engine. Quantifications were done using the algorithm integrated into MaxQuant to calculate label-free quantification intensities (Appendix Supplementary Methods).

Expanded View for this article is available online.

Acknowledgements

We thank colleagues mentioned in the text for their gifts of material. We are grateful to Julia Chamot-Rooke and Mariette Matondo from the proteomic platform of the Pasteur Institute for the availability of the Orbitrap instrument and to Odile Sismeiro and Jean-Yves Coppée from the Biomics pole of the Pasteur Institute for running the sequencing libraries on the Illumina machine. We thank the members of the laboratory, notably Cosmin Saveanu and Gwenael Breard for reading the manuscript. E. Z and E.D were supported by ANR-14-CE-10-0014-01 and ANR-17-CE11-0049-01 grants from the Agence Nationale de la Recherche (ANR), respectively. This work was supported by ANR-14-CE-10-0014-01 and ANR-17-CE11-0049-01 grants, the Pasteur Institute and the Centre National de la Recherche Scientifique. B.T. was supported by a grant from the Natural Sciences and Engineering Research Council of Canada.

Author contributions

EZ, AD, BT, ED, MG, AJ and MF-R conducted the experiments, AN generated and analysed the mass spectrometry data. VK performed sequence data analyses. MF-R and AJ wrote the paper and designed the experiments. All authors reviewed the results and approved the final version of the manuscript.

Conflict of interest

The authors declare that they have no conflict of interest.

References

- Allmang C, Petfalski E, Podtelejnikov A, Mann M, Tollervey D, Mitchell P (1999) The yeast exosome and human PM-Scl are related complexes of 3' → 5' exonucleases. *Genes Dev* 13: 2148–2158
- Anderson JS, Parker RP (1998) The 3' to 5' degradation of yeast mRNAs is a general mechanism for mRNA turnover that requires the SKI2 DEVH box protein and 3' to 5' exonucleases of the exosome complex. *EMBO J* 17: 1497–1506
- Araki Y, Takahashi S, Kobayashi T, Kajiho H, Hoshino S, Katada T (2001) Ski7p G protein interacts with the exosome and the Ski complex for 3'-to-5' mRNA decay in yeast. *EMBO J* 20: 4684–4693
- Archer SK, Shirokikh NE, Beilharz TH, Preiss T (2016) Dynamics of ribosome scanning and recycling revealed by translation complex profiling. *Nature* 535: 570–574
- Arribere JA, Gilbert WV (2013) Roles for transcript leaders in translation and mRNA decay revealed by transcript leader sequencing. *Genome Res* 23: 977–987

- Brown JT, Bai X, Johnson AW (2000) The yeast antiviral proteins Ski2p, Ski3p, and Ski8p exist as a complex *in vivo*. *RNA* 6: 449–457
- Collart MA, Oliviero S (2001) Preparation of yeast RNA. *Curr Protoc Mol Biol* Chapter 13: Unit13.12
- de la Cruz J, Kressler D, Tollervey D, Linder P (1998) Dob1p (Mtr4p) is a putative ATP-dependent RNA helicase required for the 3' end formation of 5.8S rRNA in *Saccharomyces cerevisiae*. *EMBO J* 17: 1128–1140
- Defenouillère Q, Yao Y, Mouaikel J, Namane A, Galopier A, Decourty L, Doyen A, Malabat C, Saveanu C, Jacquier A et al (2013) Cdc48-associated complex bound to 60S particles is required for the clearance of aberrant translation products. *Proc Natl Acad Sci USA* 110: 5046–5051
- Doma MK, Parker R (2006) Endonucleolytic cleavage of eukaryotic mRNAs with stalls in translation elongation. *Nature* 440: 561–564
- Dziembowski A, Lorentzen E, Conti E, Séraphin B (2007) A single subunit, Dis3, is essentially responsible for yeast exosome core activity. *Nat Struct Mol Biol* 14: 15–22
- Frischmeyer PA (2002) An mRNA surveillance mechanism that eliminates transcripts lacking termination codons. *Science* 295: 2258–2261
- Fromont-Racine M, Saveanu C (2014) mRNA degradation and decay. In *Fungal RNA biology*, Sesma A, Haar T von der (ed.), pp 159–193. Basel, Switzerland: Springer International Publishing
- Guydosh NR, Green R (2014) Dom34 rescues ribosomes in 3' untranslated regions. *Cell* 156: 950–962
- Halbach F, Reichelt P, Rode M, Conti E (2013) The yeast ski complex: crystal structure and RNA channeling to the exosome complex. *Cell* 154: 814–826
- van Hoof A, Staples RR, Baker RE, Parker R (2000) Function of the ski4p (Csl4p) and Ski7p proteins in 3'-to-5' degradation of mRNA. *Mol Cell Biol* 20: 8230–8243
- van Hoof A, Frischmeyer PA, Dietz HC, Parker R (2002) Exosome-mediated recognition and degradation of mRNAs lacking a termination codon. *Science* 295: 2262–2264
- Hu W, Sweet TJ, Chamnongpol S, Baker KE, Coller J (2009) Co-translational mRNA decay in *Saccharomyces cerevisiae*. *Nature* 461: 225–229
- Ingolia NT, Ghaemmaghami S, Newman JR, Weissman JS (2009) Genome-wide analysis *in vivo* of translation with nucleotide resolution using ribosome profiling. *Science* 324: 218–223
- Kobayashi K, Kikuno I, Kuroha K, Saito K, Ito K, Ishitani R, Inada T, Nureki O (2010) Structural basis for mRNA surveillance by archaeal Pelota and GTP-bound EF1 α complex. *Proc Natl Acad Sci USA* 107: 17575–17579
- Kowalinski E, Kögel A, Ebert J, Reichelt P, Stegmann E, Habermann B, Conti E (2016) Structure of a cytoplasmic 11-subunit RNA exosome complex. *Mol Cell* 63: 125–134
- Liu Q, Greimann JC, Lima CD (2006) Reconstitution, activities, and structure of the eukaryotic RNA exosome. *Cell* 127: 1223–1237
- Malet H, Topf M, Clare DK, Ebert J, Bonneau F, Basquin J, Drazkowska K, Tomecki R, Dziembowski A, Conti E et al (2010) RNA channelling by the eukaryotic exosome. *EMBO Rep* 11: 936–942
- Milligan L, Decourty L, Saveanu C, Rappsilber J, Ceulemans H, Jacquier A, Tollervey D (2008) A yeast exosome cofactor, Mpp6, functions in RNA surveillance and in the degradation of noncoding RNA transcripts. *Mol Cell Biol* 28: 5446–5457
- Mitchell P, Petfalski E, Houalla R, Podtelejnikov A, Mann M, Tollervey D (2003) Rrp47p is an exosome-associated protein required for the 3' processing of stable RNAs. *Mol Cell Biol* 23: 6982–6992
- Mitchell P, Tollervey D (2003) An NMD pathway in yeast involving accelerated deadenylation and exosome-mediated 3'→5' degradation. *Mol Cell* 11: 1405–1413
- Nagaraj N, Alexander Kulak N, Cox J, Neuhauser N, Mayr K, Hoerning O, Vorm O, Mann M (2012) System-wide perturbation analysis with nearly complete coverage of the yeast proteome by single-shot ultra HPLC runs on a bench top orbitrap. *Mol Cell Proteomics* 11: M111.013722
- Parker R (2012) RNA degradation in *Saccharomyces cerevisiae*. *Genetics* 191: 671–702
- Pelechano V, Wei W, Steinmetz LM (2015) Widespread co-translational RNA decay reveals ribosome dynamics. *Cell* 161: 1400–1412
- Robinson JT, Thorvaldsdóttir H, Winckler W, Guttman M, Lander ES, Getz G, Mesirov JP (2011) Integrative genomics viewer. *Nat Biotechnol* 29: 24–26
- Schmidt C, Kowalinski E, Shanmuganathan V, Defenouillère Q, Braunger K, Heuer A, Pech M, Namane A, Berninghausen O, Fromont-Racine M et al (2016) The cryo-EM structure of a ribosome-Ski2-Ski3-Ski8 helicase complex. *Science* 354: 1431–1433
- Sidrauski C, Cox JS, Walter P (1996) tRNA ligase is required for regulated mRNA splicing in the unfolded protein response. *Cell* 87: 405–413
- Sparks KA, Dieckmann CL (1998) Regulation of poly(A) site choice of several yeast mRNAs. *Nucleic Acids Res* 26: 4676–4687
- Synowsky SA, Heck AJR (2008) The yeast Ski complex is a hetero-tetramer. *Protein Sci* 17: 119–125
- Toh-E A, Guerry P, Wickner RB (1978) Chromosomal superkiller mutants of *Saccharomyces cerevisiae*. *J Bacteriol* 136: 1002–1007
- Tsuboi T, Kuroha K, Kudo K, Makino S, Inoue E, Kashima I, Inada T (2012) Dom34:Hbs1 plays a general role in quality-control systems by dissociation of a stalled ribosome at the 3' end of aberrant mRNA. *Mol Cell* 46: 518–529
- Widner WR, Wickner RB (1993) Evidence that the SKI antiviral system of *Saccharomyces cerevisiae* acts by blocking expression of viral mRNA. *Mol Cell Biol* 13: 4331–4341